

# Synthesis and Evaluation of Comb-Type Copolymers Prepared via Atom Transfer Radical Polymerization as Possible Cold Flow Improvers in GTL Diesel Fuels

M. Norah Maithufi,<sup>1,2</sup> Dawid J. Joubert,<sup>2</sup> Bert Klumperman<sup>1,3</sup>

<sup>1</sup>Laboratory of Polymer Chemistry, Eindhoven University of Technology, 5600 MB Eindhoven, The Netherlands

<sup>2</sup>Sasol Technology R&D, 1 Klasie Havenga Street, Sasolburg, South Africa

<sup>3</sup>Department of Polymer Science and Chemistry, University of Stellenbosch, Matieland, South Africa

Received 29 May 2010; accepted 8 July 2011

DOI 10.1002/app.35268

Published online 3 November 2011 in Wiley Online Library (wileyonlinelibrary.com).

**ABSTRACT:** Statistical comb-type copolymers of styrene (Sty) and stearyl methacrylate (C18 MA) with varying [styrene]:[C18MA] ratios were synthesized by a controlled/living radical polymerization technique called atom transfer radical polymerization. The polymeric materials were evaluated in selected SASOL Fischer Tropsch gas-to-liquid diesels as possible cold flow improvers. Crystallization studies revealed that as the styrene content of the copolymer increased, a crystal growth inhibition mechanism was exhibited. With an increase in styrene content of the copolymer, differential scanning calorimetry and the cloud filter plugging point (CFPP) revealed a delay in

onset of crystallization and lowered CFPP, respectively, whereas low-temperature microscopy indicated modifications and size reduction of wax crystals. However, there appeared to be a styrene content, beyond which the additive's efficiency decreased. Homopolymer and copolymers with the highest styrene content led to long unfavorable needle-shaped crystals. © 2011 Wiley Periodicals, Inc. *J Appl Polym Sci* 124: 2766–2776, 2012

**Key words:** atom transfer radical polymerization (ATRP); cold flow properties; comb-type copolymers; cold filter plugging point (CFPP); GTL diesel

## INTRODUCTION

The aliphatic hydrocarbons, which are one of the major classes of compounds in middle distillates such as diesel fuels, are known to crystallize uncontrollably out of solution at low temperatures. The attraction of the waxy hydrocarbon segments toward each other due to van der Waals forces results in the formation of wax crystals. As these wax crystals grow, they lead to a 3D interlocked network of wax crystals. If left unattended, the wax crystals can grow to sizes that can clog fuel filters or even alter the paraffin content of the fuel as the remaining fuel is trapped within the 3D network structures. Engine failures in such conditions are, therefore, inevitable. These are some of the low-temperature flow problems associated with middle distillates such as diesel fuels.<sup>1–13</sup>

For a complete efficient operation of a diesel engine, various additives are added to the fuel for a number of functions. Examples of these additives include but not limited to cetane number (CN) improvers, lubricity improvers, antifoaming, cold flow improvers (CFI), and corrosion inhibitors.<sup>3</sup> Of

most relevance to the work reported herein are diesel fuels' CFIs.

CFIs are usually added to improve low-temperature performance of diesel fuels. These additives, typically polymeric materials, improve low-temperature properties of a fuel by interacting with the fuel.<sup>6</sup> In so doing, the additives interfere with the formation and growth of paraffin wax crystals, leading to modified wax crystals that are smaller and able to flow along with the fuel. Low-temperature flow problems of fuels are in such ways improved.<sup>1–3</sup>

Polymeric compositions consisting of hydrocarbon chains and polar segments are generally used as CFIs.<sup>1–20</sup> Some of the most common ones reported to effect improvement in fuels cold flow properties include copolymers of  $\alpha$ -olefins and vinyl acetate copolymers,<sup>1–3,5,6</sup> (co)polymers of alkylacrylates,<sup>7–11</sup> and copolymers of maleic anhydride.<sup>6,12</sup>

The polymers' hydrocarbon chains provide interactions with the diesel's paraffin segment, whereas the polymers' polar groups provide spacers responsible for modifying the wax crystals.<sup>3–6</sup> This results in crystal morphological changes and prevention of wax crystals from agglomerating.

There is no universal cold flow additive for all fuels; hence, the choice of cold flow additives is largely based on the additives' interaction and response with a particular fuel. A strong interaction

Correspondence to: M. Norah Maithufi (norah.maithufi@sasol.com).

between the structure and activity of the additive with the fuel, therefore, determines how effective an additive would be. The most important attribute of an efficient cold flow additive is its chemical composition and molecular design. Polymer architectures such as block- and comb-type copolymers are among the most widely used additives.<sup>1–14</sup> The molecular design of a polymeric additive should contain a crystallizable aliphatic segment, which would interact and cocrystallize with the long *n*-alkane chains of the fuel, and a noncrystallizable part, which assists in inhibiting the growth of wax crystals and can lead to the formation of smaller modified crystals that are able to flow with the fuel.<sup>6</sup> Various operational mechanisms of additives' crystallization modifications have been reported<sup>1–7</sup> and largely point to additives being either crystallization nucleating agents or crystal growth inhibitors. In some instances, a third mechanism is observed whereby a crystal repulsion or dispersion mechanism is operational. The wax crystals are, therefore, prevented and limited from agglomerating and settling to the bottom of storage containers.<sup>1–3</sup>

The work presented here aims at evaluating the effect of varying styrene content in ATRP synthesized statistical copolymers bearing pendant long chains of C18 methacrylate (C18MA), as potential CFIs in diesel fuels. Although the investigation of cold flow additives in diesel fuel is an applied science, in this contribution, a more scientific approach is used to establish structure–property relationships.

Copolymers of (meth)acrylates are known from literature to be effective flow improvers for some fuels.<sup>7–11</sup> It was, therefore, of interest to investigate the performance of such related polymeric materials; more importantly, those prepared via the ATRP technique in GTL diesel fuels. ATRP was the polymerization technique of choice because of its ability to prepare copolymers with predetermined molecular weights, desired topologies, and control over the polymerization.<sup>15,16</sup>

The copolymers were characterized by nuclear magnetic resonance (NMR) spectrometry and size exclusion chromatography (SEC). Their performance as CFIs was evaluated in two Sasol Fischer Tropsch (FT) GTL diesel fuels, herein referred to as GTL01 and GTL02. The diesel fuels were analyzed using gas chromatography (GC), 2D-GC (GCxGC), and <sup>13</sup>C nuclear magnetic resonance (NMR) spectrometry.

## EXPERIMENTAL

### Materials

The chemicals used in this study were purchased from Sigma–Aldrich and used as received unless stated. Stearyl methacrylate was purified according

to a literature report.<sup>17</sup> Cu(I)Br was purified according to published procedure.<sup>18</sup> Anisole was passed through activated neutral alumina column and stored over molecular sieves. Styrene was passed through an activated neutral alumina column to remove inhibitors, then stored over molecular sieves and kept under nitrogen at  $-5^{\circ}\text{C}$  before use.

### Polymerizations

Ethyl 2-bromo-2-isobutyrate (EBriBu) was used as the initiator, while the monomers were styrene and stearyl methacrylate.

Polymerization of styrene and stearyl methacrylate was carried out at ratios of the [monomers]:[initiator]:[metal salt]:[ligand] = [60] : [1] : [1] : [2], under nitrogen atmosphere. A typical statistical copolymerization experiment of the monomers styrene and stearyl methacrylate (C18MA) was carried out at ratios of the [initiator]:[metal salt]:[ligand] = [1] : [1] : [2] under Schlenk conditions. The desired molecular weights and the ratios of each monomer feed were predetermined. By varying the initial monomers to initiator ratio, the final average molecular weight can be estimated using the formula  $DP_n = \Delta[\text{Monomer}]/[\text{Initiator}]_0$ .

Calculated amounts of metal salt CuBr and the ligand PMDETA in a 1 : 2 mol ratio combination of metal salt to ligand were dissolved and allowed to stir in anisole in a Schlenk flask under nitrogen atmosphere. This was followed by addition of Aliquat 336<sup>15,16</sup> as the catalyst additive at equivalent ratio to the ligand. Styrene and stearyl methacrylate were then added to the catalyst complex solution, followed by the addition of ethyl 2-bromopropionate. The flask was then immersed in an oil bath heated at  $90^{\circ}\text{C}$ . Samples of the polymerization mixture were withdrawn at different time intervals to follow kinetics. The polymers were purified by passing them through an activated neutral alumina column, followed by precipitation in cold methanol and filtration. The polymers were dried in a vacuum oven at  $50^{\circ}\text{C}$  overnight. Monomer conversion was determined gravimetrically. The copolymers' chemical compositions were confirmed by <sup>1</sup>H-NMR, indicating the presence of both the aromatic and the aliphatic segments. Representative NMR spectra for the copolymers are illustrated in Figure 1. Molecular weights and molecular weight distributions as obtained from SEC (data are illustrated in Table I).

The copolymers were assigned a generalized code indicating the copolymers composition, starting with stearyl methacrylate (C18 methacrylate) then followed by styrene molar content. A code PC18MASt16 for example signifies a Poly(C18MethAcrylateStyrene) with 16 styrene molar feed.

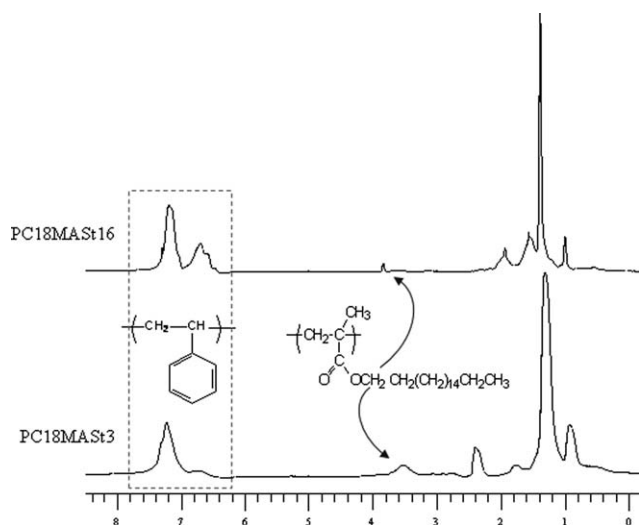


**Figure 1** Representative  $^1\text{H-NMR}$  spectra for some of the random copolymers used in this study, PC18MASt3 and PC18MASt16.

### Size exclusion chromatography

Molecular weights and molecular weight distributions were estimated using a SEC system equipped with a Waters autosampler. The polymer solution was diluted in THF to a concentration of  $\sim 1$  mg/mL. The solution was filtered over a  $0.2 \mu\text{m}$  poly(tetrafluoroethylene) syringe filter. The analysis was carried out using a Waters 2695 Alliance pump and injector, a model 2996 photodiode array detector (at 305 and 470 nm) and a model 410 refractive index detector. The columns used were two PLgel Mixed-C (Polymer Laboratories,  $5 \mu\text{m}$  particles)  $300 \times 7.5 \text{ mm}^2$  followed by a PLgel Mixed-D (Polymer Laboratories,  $5 \mu\text{m}$  particles)  $300 \times 7.5 \text{ mm}^2$  in series (which were maintained at  $40^\circ\text{C}$  for analysis). THF was used as an eluent (flow rate  $1.0 \text{ mL/min}$ ).

### Nuclear magnetic resonance

NMR experiments were performed on a Varian UNITY INOVA 400 MHz spectrometer (SMM Instruments (Pty) Ltd, South Africa) equipped with a

switchable 5 mm PFG probe in  $\text{CDCl}_3$  with TMS as the internal standard.

### Differential scanning calorimetry

Differential scanning calorimetry (DSC) studies were performed in aluminum-sealed pans using TA Q200 Universal Analysis Instrument V4.3A (AMS Laboratory Technologies). About 10 mg of solution sample was cooled from  $30^\circ\text{C}$  to  $-60^\circ\text{C}$  at a rate of  $10^\circ\text{C/min}$  and heated to  $30^\circ\text{C}$  at the same rate. The heating and cooling experiments were carried out under nitrogen atmosphere.

### Low-temperature optical microscope

Crystal morphologies were observed using an Olympus BX51 microscope (Wirsam Scientific and Precision Equipment(Pty) Ltd). Images were captured using an Olympus U-SPT Colorview camera connected to a computer. The software program AnalySIS Image Processing was used to process the data. Temperature control was performed using a Linkam TMS 94. The samples were first heated to  $20^\circ\text{C}$  then cooled to  $-50^\circ\text{C}$  using liquid nitrogen, at a rate of  $10^\circ\text{C/min}$  and heated again to  $20^\circ\text{C}$  at the same rate. Images were taken at timed intervals.

### Cold filter plugging point

Tests were done using the Institute of Petroleum (IP) Standard Methods for the analysis and testing of petroleum products, method IP 309.

### Pour point

Tests were done using the petroleum standards, according to the American Society for Testing and Materials (ASTM), method ASTM D97.

### Fuel composition

The diesel fuels used (GTL01 and GTL02) were supplied by Sasol Technology Fuels Research. The fuels

**TABLE I**  
Molecular Weight Data of the Polymeric Additives Used, Determined by SEC Against PMMA Standards. (\*Composition Based on Molar Concentration of (co)monomers Used)

Polymeric additive	Comonomer feed composition [Styrene] : [C18MA]	Molecular weight (SEC)		
		$M_n$	$M_w$	Polydispersity (PDI)
PC18MASt0	0 : 1	10,600	16,600	1.50
PC18MASt1	1 : 1	16,300	32,000	1.46
PC18MASt3	3 : 1	10,200	19,500	1.50
PC18MASt5	5 : 1	9,500	18,800	1.45
PC18MASt16	16 : 1	10,600	15,800	1.44

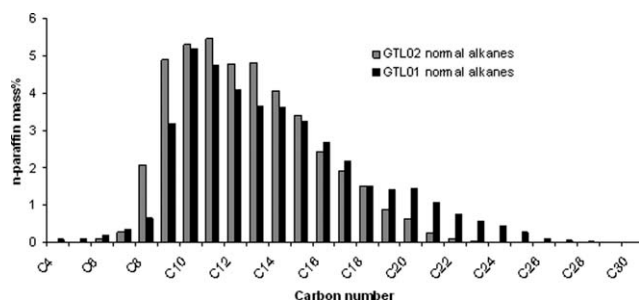


**Figure 2** Paraffin length distribution for GTL01 diesel and GTL02 diesel, data obtained by GC.

were characterized by a comprehensive multidimensional Leco Pegasus 4D GCxGC-TOF/MS system (LECO South Africa Pty. Ltd).

## RESULTS AND DISCUSSION

### Analyses of diesel fuels

Properties of diesel fuels that strongly impact engine performance include characteristics such as distillation curve of the fuel, chemical composition (*e.g.* the content of hydrocarbons and their ratio of normal to branched), aromatic content, viscosity, density, sulfur content and emissions.<sup>19,20</sup> High content of longer chain linear paraffins in diesel fuels generally lead to good CNs but can conversely compromise cold flow properties.<sup>19</sup> CN is a performance rating, which measures the ease of combustion of a diesel as indicated by the delay between the start of injection and the ignition of the fuel. Cetanes are unbranched open-chain alkane molecules that are easily ignitable under compression. The proportion of normal and isoparaffins needs to be jointly considered for good engine performance.

Figures 2–4 are depictions of major components found in the two diesel fuels. In Figure 2, the diesels' *n*-paraffin distributions are outlined, whereas Figure 3 depicts the comparison between the two diesels' normal paraffins versus branched paraffins. Figure 4 shows GCxGC contour plots illustrating the major component classes.

Figure 2 compares the paraffin mass percent of GTL01 and GTL02. The carbon numbers range from C4–C29 for GTL01, whereas the range for GTL02 is C5–C23. Generally, paraffins' solubility in the fuel decreases with increasing carbon number. A predominance of paraffins with high carbon numbers in GTL01 would indicate increased solubility problems and its intrinsic poorer cold flow properties. Figure 2, therefore, suggests that GTL02 diesel is expected to have comparatively superior cold flow properties than GTL01, as the former has moderately high carbon chain lengths.

Figure 3 denotes the comparison between the two fuels' isoparaffins. From the figure, it is noticeable that GTL01 diesel has a higher percentage of higher carbon number branched alkanes compared to GTL02.

Paraffins that are highly branched generally give rise to better cold flow properties compared to linear paraffins. The position of the branching, however, also plays a significant role in the cold flow properties of the fuel, and this simultaneously has influence on other operational parameters such as CN.<sup>3</sup>

Figure 4 is a representative GCxGC plot for the two fuels. In a 2D-GC (GCxGC) experiment, individual components are separated and grouped according to different classes such as branched and normal paraffins, cyclic paraffins, and aromatics. The technique provides a two-dimensional separation of components in complex mixtures.

GCxGC analyses of the GTL sample confirmed that GTL diesel is characterized by a highly branched paraffinic mixture in the carbon number range of C4–C30. The fuels are largely made up of normal and branched paraffins with no traceable cyclic paraffins, bicyclic paraffins, or aromatics. GTL diesel fuels display exceptional properties such as lower sulfur contents, aromatic content, and higher CN.<sup>20,21</sup> Depending on the *n*-paraffin content, the cold flow properties of GTL diesels may be compromised.<sup>20,21</sup> The responsiveness of a fuel to CFIs have been reported to be related to the *n*-paraffin content and the aromatics content.<sup>12</sup> Low *n*-paraffin contents and relatively high aromatics contents can improve the cold flow of a fuel.<sup>8,12</sup> Low *n*-paraffin contents can lead to improved low-temperature properties, while the presence of aromatics can improve the solubility of both the wax and the additives in the fuel.

The investigations reported herein aim to evaluate structural influences and interactions, of the selected copolymers of C18 methacrylate (C18MA) with varying styrene content in two GTL fuels of interest. Crystallization modifications and cold flow properties of the copolymers in diesel fuels were followed

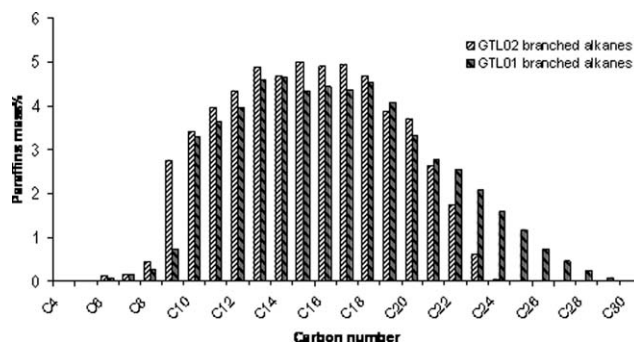


**Figure 3** Branched alkanes comparison for GTL01 and GTL02 diesel fuels, data obtained by GC.

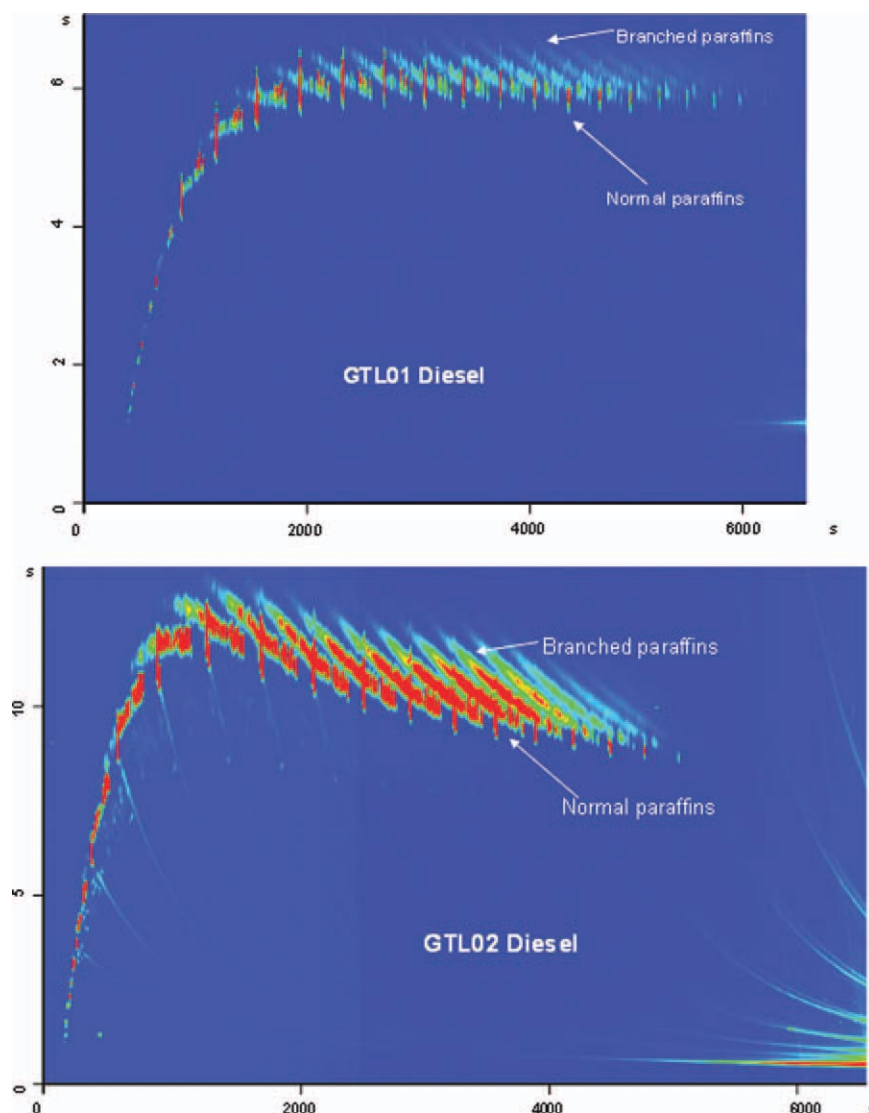


**Figure 4** GCxGC contour plots for GTL01 (a) and GTL02 (b) diesel fuels. [Color figure can be viewed in the online issue, which is available at [wileyonlinelibrary.com](http://wileyonlinelibrary.com).]

using DSC, low-temperature optical microscopy, Cold filter plugging point (CFPP), and Pour Point (PP) tests.

#### Evaluation of statistical comb-type copolymers as CFIs in GTL01 diesel fuel

Additive concentrations of 250, 500, and 1000 ppm of the studied statistical copolymers of styrene (non-crystallizable section) and C18MA (crystallizable fraction) in diesel were prepared. As shown in Table I, the copolymers differed in the [styrene]:[C18MA] comonomers molar feed, from noncrystallizable component to the highest content of 16 styrene molar content, as designed and tailored by ATRP

experimental conditions. ATRP, a controlled living radical polymerization technique allows the synthesis of polymeric materials with predetermined molecular weights, composition, and molecular architecture from different monomers such as the monomers used in this study viz. (meth)acrylates and styrenes etc.<sup>15,16</sup> ATRP experiments of the systems studies indicated a good control over the polymerization since molecular weights increased linearly with increasing monomer conversions as well as the calculated molecular weights were in agreement with the obtained experimental values. Dispersities ( $\bar{D}$ ) were maintained within 1.0 to 1.5 range and decreased with monomer conversions as expected and complying with ATRP principles.<sup>17,18</sup>

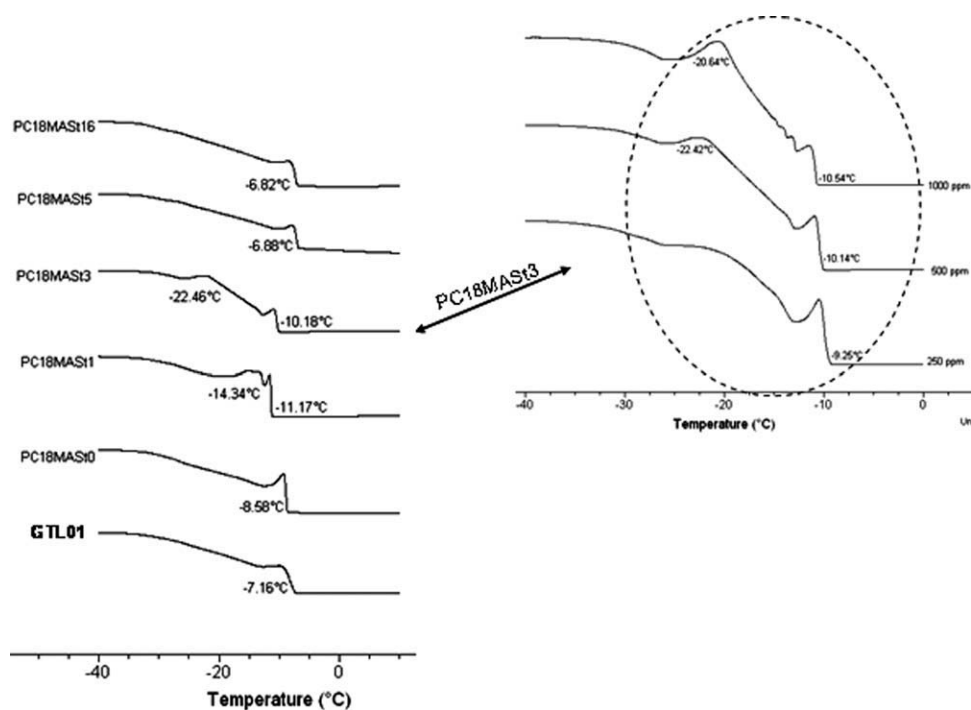


**Figure 5** DSC crystallization traces comparing copolymers of styrene and C18MA monomers at 500ppm in GTL01 diesel. The insert figure illustrates comparative crystallization traces at different additive concentrations for PSMAS<sub>3</sub>.

The rather long aliphatic chains of the monomers are known to pose solubility concerns due to their nonpolar properties in generally used polar solvents.<sup>15</sup> This can result in a slow initiation step which result in rather large dispersities.

Figure 5 outlines crystallization traces obtained from DSC of the four studied copolymers in GTL01 diesel.

Figure 5 indicates that PC18MASt<sub>1</sub> and PC18MASt<sub>3</sub> delayed the onset of crystallization ( $T_c$ ), of the diesel fuel. This delay in crystallization temperature is improved as the styrene concentration increased from zero (PC18MASt<sub>0</sub>) until PC18MASt<sub>3</sub>. The observed suppressed onset of crystallization suggests that the polymeric additives are depressing the cloud point. The crystallization mechanism via crystal growth inhibition mechanism is thus supported.<sup>2,10,11,22,23</sup> The crystal growth inhibition mechanism can be loosely explained as the process where the additive interacts with wax in a way as to prevent or delay wax from cocrystallizing with each other.<sup>10,11,22,23</sup> The affinity of wax crystals to crystallize together and form a large matrix of ordered structures is thus minimized. The resulting wax crystals are reduced in size, structurally modified, and able to flow with the fuel.<sup>2,10,11</sup>

The DSC traces indicate that  $T_c$  is suppressed by about 3 to 4° from  $-7^\circ\text{C}$  to  $-11^\circ\text{C}$  and  $-10^\circ\text{C}$  for PC18MASt<sub>1</sub> and PC18MASt<sub>3</sub>, respectively.

GTL diesel fuels, as elucidated earlier, are rich in long-chain *n*-alkanes and branched alkanes. As the

alkane molecules are in constant motion in the fuel, they can aggregate together or interact with other molecules in the matrix. Crystal growth inhibition is observed when the mobile diesel alkanes selectively associate and partition themselves toward the polymeric additive's crystallizable fractions. Because of the association with the additive, the wax molecules would then be less available to aggregate together. Wax molecules' cohesive energy (which is the force responsible for the structure ordering as described by Jang et al.<sup>10</sup>) would, therefore, be significantly lowered. The result is a slowing down of wax crystal formation and a subsequent lowering of the onset of crystallization, as observed from the DSC results (Fig. 5). Wax inhibition mechanisms using comb-type acrylate polymers have been extensively investigated by Jang et al.<sup>10</sup> and Duffy and Rodger<sup>11</sup> using molecular dynamics simulations.

Observed from this study, upon a further increase of styrene content beyond [St]:[C18MA] = 3 : 1, the polymeric additives start behaving in a similar way as both the untreated diesel fuel and the homopolymers, poly(C18MA). This was indicated by their  $T_c$ s being very similar, signifying a decline in the polymeric additive's efficiency.

Also, noticeable from Figure 5 is the two separate crystallization activities for traces PC18MASt<sub>1</sub> with [St]:[C18MA] = 1 : 1 and PC18MASt<sub>3</sub> with [St]:[C18MA] = 3 : 1. In the latter case, the difference between the first and second crystallization peak is more than 10°, whereas in the former, this difference

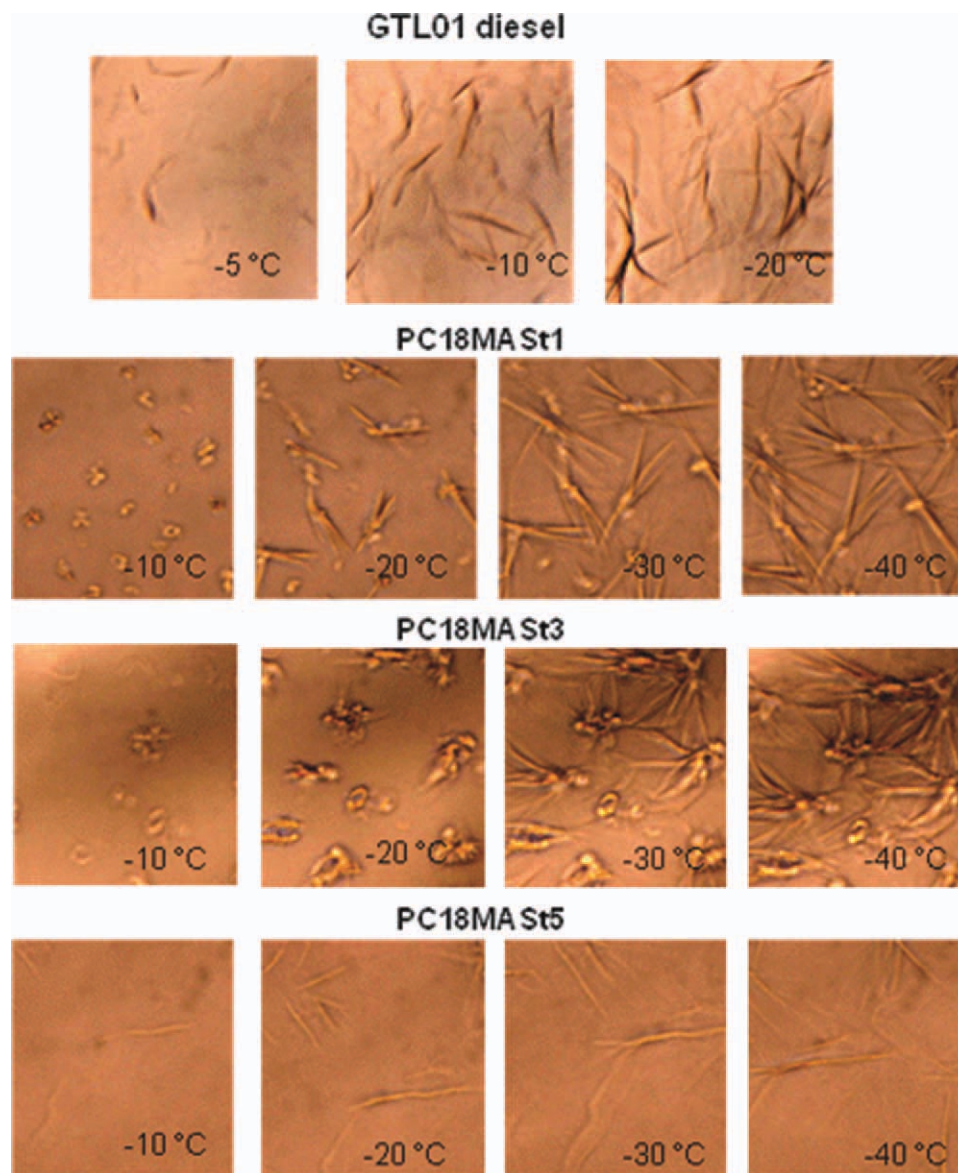


**Figure 6** Micrographs illustrating evolution of crystal formation over temperature in GTL01 diesel treated with 500 ppm of C18MA-styrene random comb copolymers. Image size  $50 \times 50 \mu\text{m}^2$ . [Color figure can be viewed in the online issue, which is available at [wileyonlinelibrary.com](http://wileyonlinelibrary.com).]

is only a few degrees. It is postulated that with these additives, as the temperature is lowered further there could still be some wax molecules which did not have sufficient association with the polymeric additive in the primary crystallization. These molecules are likely to be shorter alkanes as they crystallize only at much lower temperatures. At higher additive concentrations, the extent of this secondary crystallization was more pronounced. The insert in Figure 5 indicates this observation, with 1000 ppm concentration showing the largest secondary crystallization activity as denoted by a larger area under the crystallization peak at around  $-20^\circ\text{C}$ . The area under a crystallization peak is generally proportional to the crystal mass formed, based on the enthalpy of crystallization.<sup>24</sup>

An increase in additive's concentration provided more crystallization nucleating sites for the unassociated wax molecules to further crystallize. The fuel treated with 250 ppm additive behaved quite similar to the untreated diesel, with crystallization not significantly altered. The area under the crystallization peak for the fuel treated with 250 ppm additive is larger than that for the untreated diesel. This suggests that 250 ppm concentration of the polymeric additive in diesel is not efficient to effect positive low-temperature properties. A similar trend was observed from the microscopy studies, illustrated in Figure 6.

Figure 6 depicts micrographs of GTL01 treated with the additives PC18MASt1, PC18MASt3, and PC18MASt5 at 500 ppm individually. Crystal

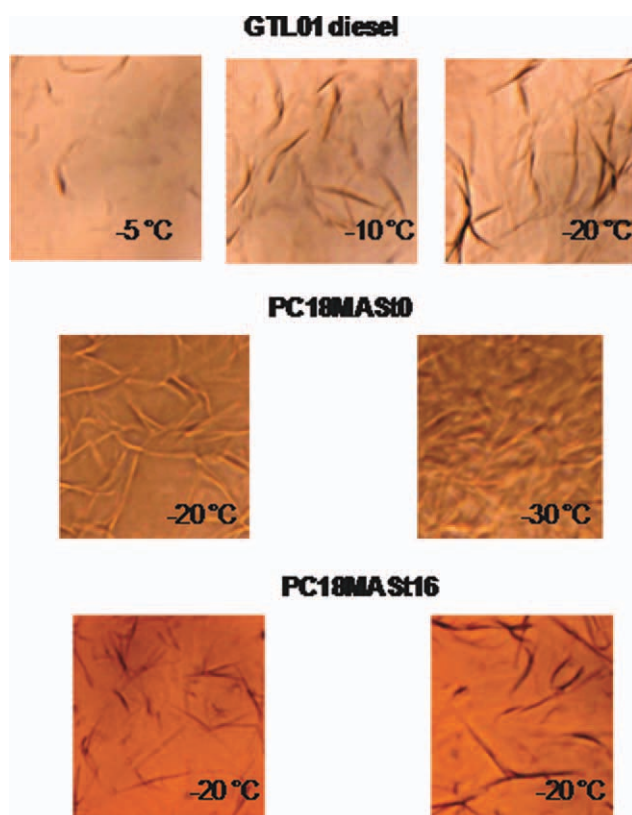


**Figure 7** Micrographs for the homopolymers of C18MA with no styrene (PC18MASt0) and the polymer with the high-styrene content (PC18MASt16), illustrating evolution of crystal formation over temperature in GTL01 diesel treated with 500 ppm of the polymers. Image size  $50 \times 50 \mu\text{m}^2$ . [Color figure can be viewed in the online issue, which is available at [wileyonlinelibrary.com](http://wileyonlinelibrary.com).]

morphologies observed for PC18MASt3 were spherulitic-type crystals at the beginning, which upon further cooling appear to be deformed by needle-type protrusions onto the spherulites (Fig. 6 bottom micrographs). This behavior differs markedly from that shown by the crystallization patterns of the untreated diesel over temperature (Fig. 6 top micrographs), which appeared as large plate-like crystal morphology.<sup>25–30</sup>

Apparent from Figure 6 is that the untreated diesel rapidly formed agglomerated crystals earlier on over the experimental temperature range. This phenomenon is common for untreated diesel that a 3D network forms and it is the reason for flow problems.<sup>1–14,25–31</sup> Addition of the polymers displayed modifications to the wax crystal morphologies. Also evident from microscopy, different polymeric additives induced varying crystal morphologies. PC18MASt1 and PC18MASt3 had similar crystal morphologies. Crystal morphologies of these two copolymers, however, were distinctly different from the third evaluated polymeric additives (PC18MASt5). PC18MASt1 and PC18MASt3, there-

fore, indicated their comparable crystallization mechanisms.

As the temperature was lowered further, the earlier mentioned long needle-like extensions were observed. It is conceivable that at these lower temperatures, the unassociated wax molecules would be crystallizing out of solution and using the already formed crystals as crystallization site, thus appearing as the above explained needle-like extensions.<sup>25</sup> Polymers with the highest styrene content (PC18MASt16) and the homopolymer of C18MA (PC18MASt0) were inefficient in improving cold flow properties of GTL01. Unfavorably, long crystals of more than  $40 \mu\text{m}$  were obtained.

Figure 7 depicts the crystals observed from the C18MA homopolymer, PC18MASt0 and the highest styrene content copolymer, PC18MASt16. The figure shows that at  $-20^\circ\text{C}$ , a significant amount of the undesired long needle-like crystal materials is already noticeable. Clearly different from the almost spherical crystals of PC18MASt1 and PC18MASt3 shown in Figure 6; crystal morphologies of PC18MASt0 and PC18MASt16 in GTL01 are very long and large undesirable crystals.

Attempts to investigate crystallization behaviors of various homopolymers of styrene could not be pursued due to solubility problems of polystyrene in the investigated diesel fuels. Different homopolymers of styrene prepared under similar ATRP conditions as the evaluated polymers reported herein exhibited the worst solubility in the fuels investigated. The polymers precipitated out of solution; crystallization studies for the styrene homopolymers in the diesel fuels were thus unsuccessful.

The observations from the crystallization studies strongly suggest and support the significance of chemical composition of additives and the resultant interactions with the fuels. The results also confirm that, for the investigated fuel, appropriate proportions of both the crystallizable and noncrystallizable fractions of the polymeric additive are equally significant components governing the overall efficacy of the additive in improving low-temperature properties.

### Cold filter plugging point and pour point

CFPP and PP experiments were carried out for the four statistical copolymers used in this study at 500 ppm polymeric additive in both GTL01 and GTL02 diesel fuels. It is generally known that cold flow additives respond differently to different solvents; therefore, a comparative evaluation was pursued in these different diesel fuels to establish the extent of the variations between the two fuels. Table II outlines the CFPP and PP results.

Interesting from Table II is the noticeable minimal influence of the copolymers on GTL02, as neither



**TABLE II**  
**CFPP and PP Results in GTL01 and GTL02 Diesel Fuels**

	GTL01		GTL02		
	CFPP (°C)	PP (°C)	CFPP (°C)	PP (°C)	
Untreated GTL01	-5	-12	Untreated GTL02	-20	-21
PC18MASt0	-6	-12	PSMASt0	-19	-24
PC18MASt1	-10	-9	PSMASt1	-17	-24
PC18MASt3	-10	-9	PSMASt3	-20	-24
PC18MASt5	-5	-9	PSMASt5	-20	-21
PC18MASt16	-5	-9	PSMASt16	-20	-21

CFPP modifier nor PP modifiers. Because GTL02 already has quite low CFPP and PP, it is projected that it would be more challenging to improve on the flow properties of this diesel. GTL02 was, therefore, a harder-to-treat diesel fuel.<sup>18</sup> GTL01 on the other hand showed a positive interaction with PC18MASt1 and PC18MASt3, where a  $\Delta$ CFPP of  $-5^{\circ}\text{C}$  was obtained. This observation extends to the earlier DSC and microscopy discussions relating to the crystallization mechanism of the two copolymers in GTL01. The copolymers did not show a positive influence on PP for both GTL fuels. Pour point depressants (PPDs) are additives that are able to reduce the PP and improve flow properties of fuels.<sup>3,31</sup> The mechanism for PPDs, although not clearly understood, has been related to disruption and prevention of network formation of wax crystals by adsorption of the PPD onto the wax crystal.<sup>31</sup> PP additives are not involved in altering wax crystal formation but are involved with the already formed crystals by adsorption onto the wax crystal via intermolecular forces.

In their study, Abdel Azim et al.<sup>31</sup> demonstrated the effect of styrene content. They found that increasing the styrene content had a negative effect on the performance of the copolymers as PP additives. Copolymers with high styrene contents led to poor pour point depression due to the phenyl ring

reducing the adsorption of the additive onto wax crystals. Analogous to our study, increasing the styrene content of the copolymers was found to have a deteriorating effect on the performance of the copolymers. With regard to the homopolymer (PC18MASt0), it is speculated that the polymer energetically favors to self-assemble such that the wax molecules are, therefore, unable to interact with the polymers. Without interaction with wax molecules, the homopolymer would then precipitate out of solution leaving the wax molecules to cocrystallize with each other leading to the undesired wax crystals that cause low-temperature flow problems.<sup>19</sup>

#### Proposed crystallization mechanism of statistical comb-type PC18MASt copolymers in GTL01 and GTL02 diesel fuels

As described throughout the communication, paraffin waxes tend to form orderly stacked crystals at low temperatures that cause low-temperature flow problems. Based on this study, it is conceivable that the statistical comb copolymers facilitated an association between wax molecules the polymers, thereby leading to paraffin crystals being less available to crystallize and coaggregate together. Consequently, this led to a delay in the onset on crystallization and the observed lowered CFPP.

The presence of randomly incorporated long chain alkyl groups of the copolymer allowed for the crystallizable fractions of both the fuel and the copolymer to associate with each other. The noncrystallizable bulky styrene groups acted as spacers in between the long methacrylate units. The spacer units prevent and disrupt long alkyl chains of the polymer from self-aggregation, which could result in decreased interaction with the paraffin molecules. Too low or too high contents of the styrene units were detrimental because solubility was then compromised, leading to the polymeric additive precipitating out of the fuel.

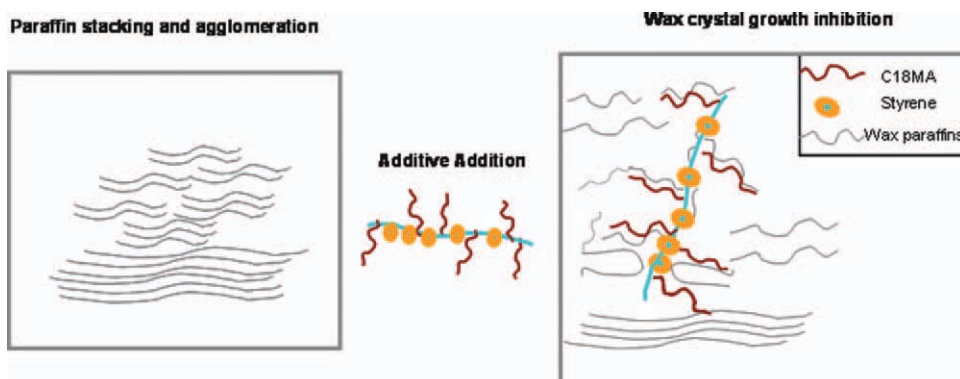


**Figure 8** Schematic depiction of operating mechanism for the random copolymers in diesel fuels. This scheme was adapted from Ref. 10. [Color figure can be viewed in the online issue, which is available at [wileyonlinelibrary.com](http://wileyonlinelibrary.com).]

Figure 8 attempts to illustrate the proposed interaction mechanism between the polymeric additive and the paraffin segments of the diesel.

## CONCLUSIONS

Statistical comb-type copolymers of styrene and stearyl methacrylate were prepared via a controlled/living radical polymerization, ATRP, and evaluated for their crystallization modification properties in Sasol FT Gas-To-Liquid diesel fuels as possible CFIs.

The results signified the importance of chemical composition of additives and their resultant interactions with the fuels. Crystallization studies from DSC confirmed a delay in the onset of crystallization. Crystal morphological changes and reduction in crystal size observed from low-temperature optical microscopy further supported positive interactions between the polymers and the diesel.

Crystallization studies revealed that an increase in the styrene content of the copolymers induced a crystal growth inhibition mechanism as evidenced by a suppressed  $T_c$  of about 3°C. However, beyond [St]:[C18MA] = 3 : 1, the polymeric additives lose efficiency. This was indicated by  $T_c$  being very similar to the untreated diesel, thus signifying a decline in the polymeric additive's efficiency.

The results substantiate the notion that an efficient cold flow additive requires the presence and appropriate compositions of the crystallizable (to interact with the wax paraffin fraction) as well as the non-crystallizable fractions (to disrupt and hinder crystal growth) in the evaluated GTL diesel fuels.

The lowered CFPP corroborated crystallization results observed from DSC and low-temperature optical microscopy. CFPP results indicated positive effects of [St]:[C18MA] = 1 : 1 and [St]:[C18MA] = 3 : 1, beyond which the loss of the polymers' efficiency was noticed.

Results from various analyses performed throughout the study are consistent with the fact that there appears to be a styrene content, beyond which the polymers' efficiency decreases. For these systems, [St]:[C18MA] = 3 : 1 seemed to be that composition.

Homopolymer of poly(C18MA) and copolymers with the highest styrene content led to long undesirable needle-shaped crystals. Attempts to investigate crystallization behaviors of various homopolymers of styrene could not be pursued, as the polymers were insoluble in the investigated diesel fuels.

The evaluated copolymers did not display good PPDs properties as PPs of both GTL01 and GTL02 were not reduced by the presence of the copolymers.

Also, none of the investigated polymers positively influenced GTL02 diesel's cold flow properties. The different chemical compositions of the two fuels suggest that they interact differently with the investigated copolymers. The influence and effect of the polymeric additives are, therefore, fuel specific.

The authors thank, Sasol Technology (Pty) Ltd for permission to publish this work, Sasol Technology Fuels Research for the kind donation of the diesel fuels and the opportunity to pursue this study, Rina van der Westhuizen (Sasol Technology R and D) for the diesel fuels analyses, Mr. Musa Mthombeni (Sasol Technology R and D) for lab assistance, Dr Alpheus Mautjana and Mr. Gareth Bayley (Stellenbosch University) for SEC analyses. Prof Bert Klumperman acknowledges support by the South African Research Chair Initiative (SARChI) of the DST and NRF.

## References

1. Marie, E.; Chevalier, Y.; Brunel, S.; Eydoux, F.; Germanaud, L.; Flores, P. *J Colloid Interface Sci* 2004, 269, 117.
2. Marie, E.; Chevalier, Y.; Eydoux, F.; Germanaud, L.; Flores, P. *J Colloid Interface Sci* 2005, 290, 406.
3. Ribeiro, N. M.; Pinto, A. C.; Quintella, C. M.; da Rocha, G. O.; Teixeira, L. S. G.; Guarieiro, L. L. N.; do Carmo Rangel, M.; Veloso, M. C. C.; Rezende, M. J. C.; da Cruz, R. S.; de Oliveira, A. M.; Torres, E. A.; de Andrade, E. A. *Energy Fuels* 2007, 21, 2433.
4. Guo, X.; Pethica, B. A.; Huang, J. S.; Prud'homme, R. K.; Adamson, D. H.; Fetters, L. J. *Energy Fuels* 2004, 18, 930.
5. Machado, A. L. C.; Lucas, E. F.; González, G. *J Pet Sci Eng* 2001, 32, 159.
6. Guo, X.; Tinsley, J.; Prud'homme, R. K. *Prepr Pap-Am Chem Soc Div Pet Chem* 2005, 50(3), 288.
7. El-Gamal, I. M.; Atta, A. M.; Al-Sabbagh, A. M. *Fuel* 1997, 76(14/15), 1471.
8. El-Gamal, I. M.; Khird, T. T.; Ghuiba, F. M. *Fuel* 1998, 77(5), 375.
9. El-Gamal, I. M.; Ghuiba, F. M.; El-Batanoney, M. H.; Gobiél, S. *J Appl Polym Sci* 1994, 5, 9.
10. Jang, Y. H.; Blanco, M.; Creek, J.; Tang, Y.; Goddard, W. A., III. *J Phys Chem B* 2007, 111, 13173.
11. Duffy, D. M.; Rodger, P. M. *Phys Chem Chem Phys* 2002, 4, 328.
12. Zhang, H.; Liu, H.; Wang, S. *Petrochem Sci* 2009, 6, 82.
13. Ashbaugh, H. S.; Guo, X.; Schwahn, D.; Prud'homme, R. K.; Richter, D.; Fetters, L. J. *Energy Fuels* 2005, 19, 138.
14. Wu, C.; Zhang, J.-L.; Li, W.; Wu, N. *Fuel* 2005, 84, 2039.
15. Chatterjee, D. P.; Mandal, B. M. *Polym J* 2006, 47, 1812.
16. Çaylı, G.; Meier, M. A. R.; *Eur J Lipid Sci Technol* 2008, 110(9), 853.
17. Qin, S.; Saget, J.; Pyun, J.; Jia, S.; Kowalewski, T.; Matyjaszewski, K. *Macromolecules* 2003, 36, 8969.
18. Matyjaszewski, K.; Miller, P. J.; Pyun, J.; Kickelbick, G.; Diamanti, S. *Macromolecules* 1999, 32, 6526.
19. Reddy, S. R.; McMillan, L. M. SAE Technical Paper 811181, 01 October 1981.
20. Stavinoha, L. L.; Alfaro, E. S.; Dobbs, H. H., Jr; Villahermosa, L. A.; Heywood, J. B. SAE Technical Paper 2000-01-3422, 04 December 2000.
21. Leckel, D. *Energy Fuel* 2009, 231, 2342.
22. Botros, M. G. SEA Technical Paper 972899, 01 October 1997.
23. Kern, R.; Dassonville, R. *J Cryst Growth* 1992, 116, 191.

24. Cho, S. Y.; Fogler, H. S.; *J Ind Eng Chem* 1999, 5(2), 123.
25. Radulescu, A.; Schwahn, D.; Stellbrink, J.; Kentzinger, E.; Heiderich, M.; Richter, D. *Macromolecules* 2006, 39, 6142.
26. Claudy, P.; Létoffé, J.-M.; Bonardi, B.; Vassilakis, D.; Damin, B. *Fuel* 1993, 72(6), 821.
27. Létoffé, J.-M.; Claudy, P.; Vassilakis, D.; Damin, B. *Fuel* 1995, 74(12), 1830.
28. Ashbaugh, H. S.; Radulescu, A.; Prud'homme, R. K.; Schwahn, D.; Richter, D.; Fetters L. *Macromolecules* 2002, 35, 7044.
29. Schwahn, D.; Richter, D.; Lin, M.; Fetters, L. *J Macromolecules* 2002, 35, 3762.
30. Leube, W.; Monkenbusch, M.; Scheiders, D.; Richter, D.; Adamson, D.; Fetters, L.; Dounis, P.; Lovegrove, R. *Energy Fuels* 2000, 14, 419.
31. Abdel Azim, A.-A. A.; Nassar, A. M.; Ahmed, N. S.; Kamal, R. S. *Pet Sci Tech* 2006, 24, 887.